NASA Technical Paper 1722

Spectral Flame Radiance From a Tubular-Can Combustor

Russell W. Claus

FEBRUARY 1981

NASA

NASA Technical Paper 1722

Spectral Flame Radiance From a Tubular-Can Combustor

Russell W. Claus
Lewis Research Center
Cleveland, Ohio

National Aeronautics
and Space Administration

**Scientific and Technical
Information Branch**

1981

Summary

The effects of fuel type, inlet-air pressure, and fuel-air ratio on spectral flame radiance in a JT8D can combustor were investigated. Spectral radiance measurements from 1.55 to 5.5 micrometers of wavelength were recorded at three axial locations in the combustor. These measurements were analyzed to determine local values of soot concentration and flame temperature. Two fuels, ERBS (experimental referee broadened specification) and Jet-A, differing in volatility, viscosity, and chemical composition were burned at a variety of combustor operating conditions. Combustion of the ERBS fuel resulted in increased levels of spectral radiance at most operating conditions. These increased radiance levels were generally attributed to high flame temperatures. With Jet-A fuel an increase in both flame temperature and soot concentration resulted from an increase in the inlet-air pressure. With Jet-A fuel an increase in the overall fuel-air ratio did not significantly affect the primary-zone spectral radiance but did increase the spectral radiance in the secondary and tertiary zones. With the less volatile and more viscous fuel the primary-zone spectral radiance was affected by variations in the fuel-air ratio.

Introduction

An experimental investigation was conducted to determine the effects of fuel type and combustor operating condition on the spectral flame radiance emanating from a JT8D can combustor. These measurements were analyzed to determine soot concentration and flame temperature along the length of the combustor.

Calculation of the radiant heat transfer from the flame to the combustor liner wall is involved in the design of aircraft combustion systems. This heat flux largely determines the amount of air required to cool the liner, especially at high-pressure conditions. It is undesirable to use too much air to cool the liner, as the quenching effects of the cooling air can adversely affect low-power emissions. Yet at the same time the liner must be kept as cool as possible to prolong its life. Designers have compromised these two effects by using empirical flame radiation correlations, such as that developed by Reeves in reference 1, to calculate liner temperature.

In the past these empirical correlations have provided satisfactory approximations of liner temperature, but a number of current engine design trends are imposing a need for greater accuracy. First, the combustor is being designed to operate at increasingly higher pressures, where it will encounter much greater radiant heat loadings. Second, the uncertainty of future fuel supplies may result in combustors being designed to operate on less highly refined fuels. This degradation of fuel quality can, again, result in increased radiant heat loadings (refs. 2 to 4). Finally, the design of combustors to operate at higher turbine inlet gas temperatures will increase both the radiant and convective heat loadings throughout the combustor.

It is therefore necessary to calculate radiant heat fluxes more accurately than the estimates provided by Reeves' empirical correlation. Several techniques (refs. 5 and 6) that calculate flame radiation by combining the emissivities of the combustion gases and the soot particles would appear to provide the necessary accuracy. Unfortunately, conducting such calculations for gas turbine design requires foreknowledge of two main quantities: flame temperature, and soot concentration.

Presently no correlations establishing the relationship between these quantities and such combustor design variables as fuel type, fuel-air ratio, and inlet-air pressure are available. To construct such correlations requires exhaustive measurements throughout the combustor. These measurements are frequently difficult to obtain since high soot levels in the primary zone of the combustor can cause plugging of a probe inserted into the flowstream. In addition the physical disturbance of the flowfield caused by a probe may reduce the validity of the measurement. Norgren (refs. 7 and 8) has resolved this problem by employing a nonintrusive optical technique that measures flame spectral radiance at two wavelengths to determine local values of flame temperature and soot concentration. These measurements were limited to experimental combustor geometries.

The present investigation uses a variation of this optical technique to examine the effect of fuel type and combustor operating conditions on spectral flame radiance in a combustor representative of those now in commercial service. Measurements were made over a range of wavelengths from 1.55 to 5.5 micrometers, from which the local values of soot concentration and flame temperature were

calculated. Tests were conducted with Jet-A and an experimental referee broadened-specification (ERBS) fuel. The operating conditions were varied over pressures from 0.28 to 1.03 MPa, fuel-air ratios from 0.006 to 0.0155, and inlet-air temperatures from 400 to 700 K. Measurements were taken at three axial locations in the combustor.

Analysis

Total flame radiation is composed of the spectral emission of several high-temperature combustion products. The combustion gases, predominantly carbon dioxide and water vapor, emit and absorb radiant energy in discrete spectral bands. For carbon dioxide these bands are centered at wavelengths of 2.0, 2.7, 4.3, 9.4, 10.4, and 15.0 micrometers as tabulated in reference 9. Similarly, water vapor bands are centered at wavelengths of 1.38, 1.87, 2.7, and 6.3 micrometers. The individual intensity of these spectral bands varies greatly, and many are too weak to make a significant contribution to total flame radiation. For the spectral region involved in this investigation only the 2.7-micrometer band of water vapor and the 4.3-micrometer band of carbon dioxide are of interest. The other major contributor to flame radiation is soot. Soot emits a continuous spectrum the intensity of which is very much dependent on the soot concentration level.

The following sections describe the technique whereby the spectral profiles of soot and the combustion gases can be used to calculate soot concentration and flame temperature.

Flame Temperature

The flame temperature was determined by assuming that carbon dioxide radiates like a blackbody in a spectral region around 4.45 micrometers.[1] From this the flame temperature can be straightforwardly obtained from Planck's equation of spectral radiance:

$$i_{\lambda b} = \frac{2C_1}{\lambda^5 (e^{C_2/\lambda T} - 1)} \qquad (1)$$

where $i_{\lambda b}$ is the experimentally measured radiance, λ is the wavelength, T is the flame temperature, and C_1 and C_2 are constants ($C_1 = 5.954 \times 10^{-11}$ W cm^2 and $C_2 = 1.4388$ cm K).

This technique is consistent with the findings of Miller, et al. (ref. 10) in which carbon dioxide was found to exhibit blackbody radiance at 4.4 micrometers. This finding was valid over a large range of combustor operating conditions and with a variation in fuel type from iso-octane to toluene.

Further verification of the technique used to calculate flame temperature can be obtained from figure 1. Tertiary-zone gas temperature as determined from spectral radiance measurements is plotted against the average exhaust gas temperature as measured by thermocouples. A line of perfect agreement is shown in the figure. Tertiary-zone gas temperatures averaged 16 percent higher than the exhaust-gas temperatures. These higher gas temperatures are not surprising in view of the fact that a significant portion of the total airflow is being injected into the combustion gas stream near or downstream of the tertiary-zone viewing port. The effect this might have on the hot-gas profile is illustrated in figure 2. The dilution air will not have fully mixed with the combustion gases at the viewing port; and since radiation is proportional to the fourth power of temperature, the radiometer will essentially only "see" the hotter gases. So the higher tertiary-zone gas temperatures in figure 1 can be attributed to hot-gas profile distortions at the sample port.

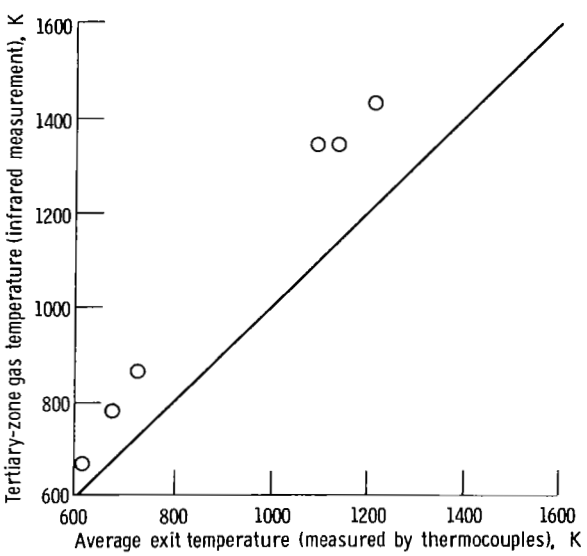

Figure 1. - Infrared measurement of tertiary-zone gas temperature as a function of exhaust-gas temperature for Jet-A fuel.

[1] The choice of 4.45 μm as the wavelength to be used in eq. (1) rather than the nominal center of the band at 4.3 μm was dictated by atmospheric absorption of spectral radiance around 4.3 μm of wavelength. The high pressure and temperature within the combustor cause collisional broadening of the carbon dioxide emission band; therefore measurement of carbon dioxide spectral radiance can be made at 4.45 μm of wavelength without concern for absorption caused by atmospheric carbon dioxide in the optical path.

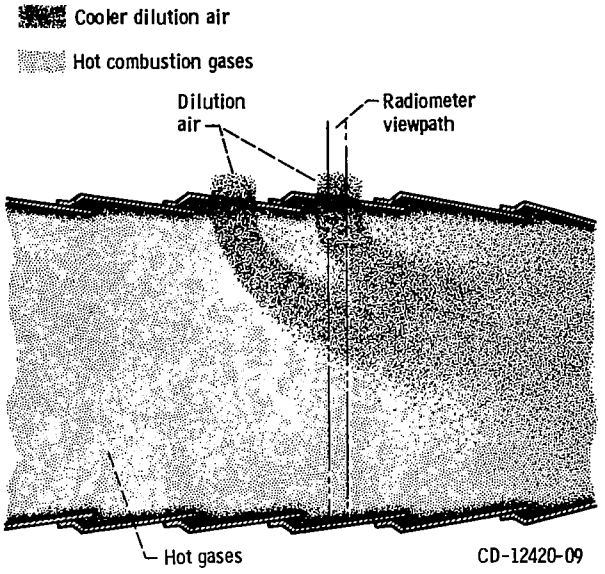

Figure 2. - Illustrative drawing of effect of dilution air on hot-gas profile in radiometer viewpath.

Note that only Jet-A data were used to construct figure 1. When ERBS fuel was combusted, the tertiary-zone temperatures were notably higher. This is probably a mixing phenomenon but may also be related to a small amount of combustion still occurring at the tertiary-zone sample port. (See the section Results and Discussion for further discussion of ERBS fuel combustion).

Soot Concentration

A cloud of soot particles emits a continuous spectrum of radiation that can be described by

$$i_\lambda = i_{\lambda b}[1 - \exp(-K_\lambda CL)] \qquad (2)$$

where i_λ is the soot spectral radiance, $i_{\lambda b}$ is the blackbody radiance at flame temperature, K_λ is the extinction coefficient, C is the soot concentration, and L is the optical path length. The subscript λ indicates a spectrally dependent quantity.

To calculate the spectral radiance of a cloud of soot particles for a given value of C, the extinction coefficient, the blackbody radiance, and the optical path length must be determined. The extinction coefficient K_λ can be calculated from Mie theory. Foster's solution, as reproduced in figure 3 (from ref. 11), is used in this analysis. Blackbody radiance $i_{\lambda,b}$ can be calculated from Planck's equation (1). Optical path length L is related to the combustor diameter and was 15 centimeters.

From these quantities equation (2) can be used to predict a curve of soot spectral radiance versus wavelength for a given soot concentration. Different values of soot concentration were chosen iteratively to match the experimentally measured spectrum with the spectrum predicted from equation (2). Gas band radiation around 2.7 and 4.3 micrometers of wavelength caused discontinuities in the experimentally measured spectrum. For this reason the matching process was performed from 1.55 to 4.0 micrometers, and a line was faired through the 2.7-micrometer gas band to eliminate the discontinuity in this region. The value of soot concentration chosen in this manner is the value reported in this investigation.

The agreement attained by this matching process is shown in figure 4. If the discrepancy caused by gas band radiation around 2.7 and 4.3 micrometers is ignored, the spectral radiance calculated from equation (2) matches reasonably well with the experimentally measured spectrum. Some disagreement can be seen at wavelengths shorter than 2 micrometers. This disagreement represents only a small portion of the total radiant heat flux and is therefore considered acceptable.

Before the iterative, matching process was used to calculate a value of soot concentration, the following assumptions were made:

(1) The representative particle size for the soot

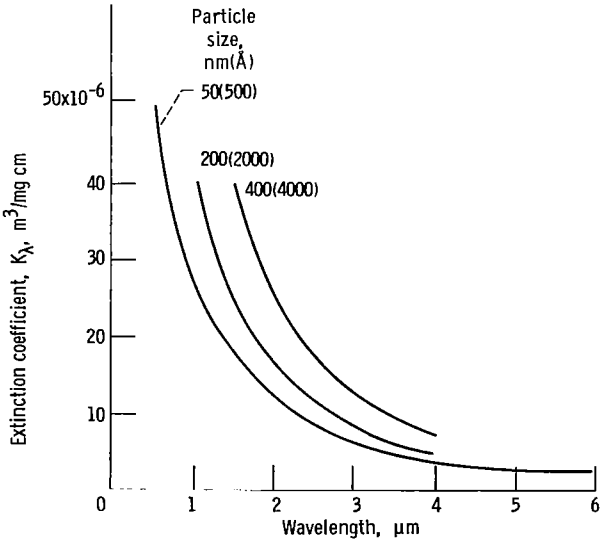

Figure 3. - Extinction coefficient of soot particles calculated from Mie theory as a function of wavelength.

cloud was 50 nanometers (500 Å) (refs. 7 and 12).

(2) The optical properties of soot are independent of both the carbon-hydrogen ratio (ref. 13) and the temperature of the soot (ref. 14).

(3) Over the optical path length in the combustor, flame temperature and soot concentration can be represented by a single value.

(4) The experimentally measured spectral radiance was due to soot particle radiation, except around the 2.7- and the 4.3-micrometer gas band regions.

The final assumption was tested before each calculation of soot concentration was made. The optical viewing path included the backside combustor liner, and at very low soot concentration levels the radiance from the liner wall was greater than the soot spectral radiance for a portion of the total measured spectrum. The liner radiance could be estimated from liner metal thermocouple readings and greybody considerations. When the estimate of liner radiance equalled any portion of the experimentally measured spectral radiance, no calculation of soot concentration was made.

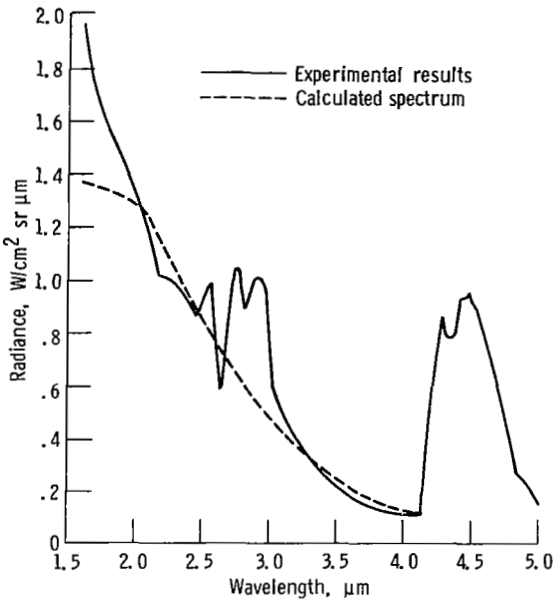

Figure 4. - Comparison of spectral radiance as predicted by Mie theory with experimentally measured values taken in primary zone of combustor, as a function of wavelength.

Apparatus

Test Facility

The test facility is shown schematically in figure 5. The preheater supplied nonvitiated air to the combustor. Pressures and flowrates were regulated by remotely controlled valves upstream and downstream of the test section. Inlet-air pressure and temperature were measured at the inlet to the combustor test section. At the combustor exit, exhaust gas temperatures were measured with eight Chromel-Alumel thermocouple rakes. Airflow rates were measured by a square-edged orifice installed according to ASTM specifications. Fuel flow rates were measured by turbine flowmeters with frequency-to-voltage converters for readout and recording.

Combustor

The JT8D can combustor used in this investigation is representative of those currently in widespread commercial service on several aircraft. The combustor features a single dual-orifice nozzle to inject fuel into the primary zone. Ten liner louvers provide film cooling along the length of the combustor. Two thermocouples were located in the middle of each liner louver to measure liner metal temperature. A number of dilution air holes distribute the airflow both to optimize combustion efficiency at all operating conditions and to provide a uniform gas temperature profile exiting the combustor. The maximum design pressure for the combustor is 1.7 MPa, corresponding to an engine pressure ratio of 16.9 to 1. Maximum design exit temperature is 1348 K.

The JT8D can combustor used in this investigation was modified to accommodate three optical viewing ports as shown in figure 6. These ports were labeled primary zone, secondary zone, and tertiary zone. These labels serve for reference purposes even though the distinction between these combustion zones in a JT8D combustor is not clear. The primary-zone, secondary-zone, and tertiary-zone optical ports were located 6, 21, and 33 centimeters, respectively, downstream of the fuel nozzle. In the tertiary zone a dilution air hole already installed on the liner was used for optical access. In the primary and secondary zones precisely alined holes had to be drilled into the liner for optical access. These holes were sized small enough to provide minimal disturbance of the airflow and large enough to accommodate thermal expansion of the combustor liner. Sapphire windows were installed on the combustor housing to allow viewing of the liner ports. The primary zone port was purged with nitrogen to keep the sapphire window free of contamination. A similar purge was not needed at the other ports.

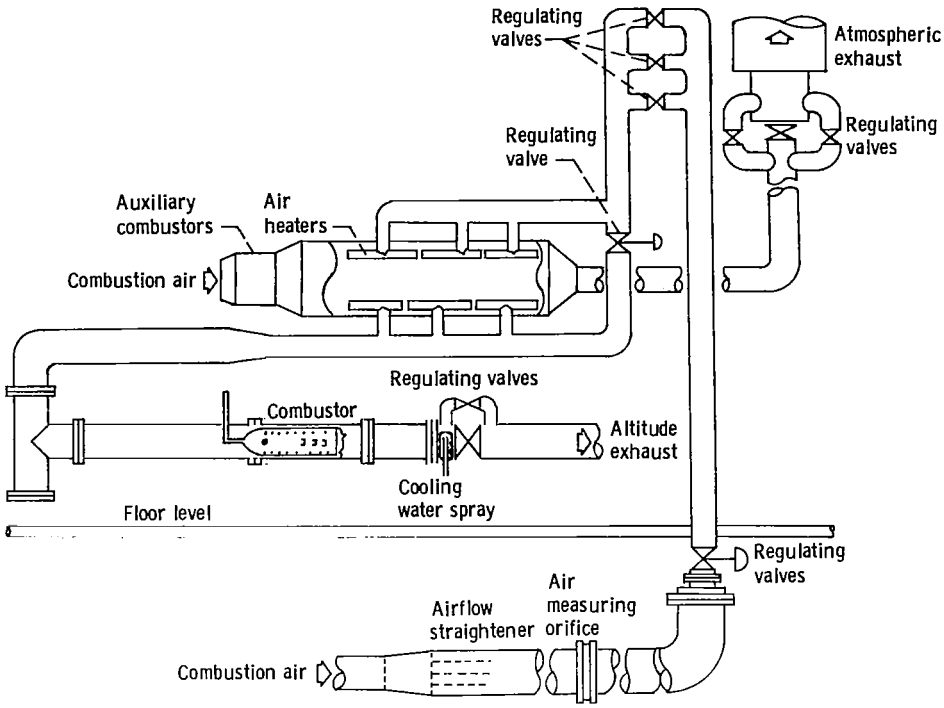

Figure 5. - Test facility and auxiliary equipment.

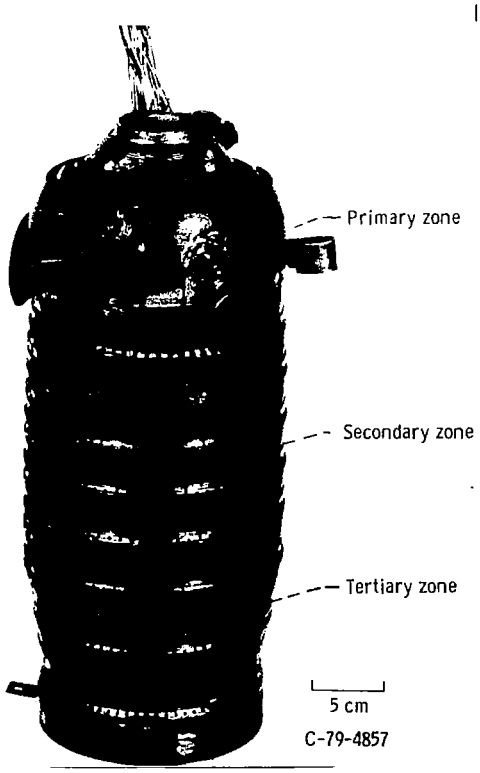

Figure 6. - JT8D combustor showing radiometer observation ports.

Fuels

The characteristics of the two fuels used in this investigation are given in table I. The specifications for the experimental referee broadened-specification (ERBS) aviation turbine fuel were established in reference 15. It was proposed that such a fuel could be produced from the available petroleum stocks without excessive processing costs. Accordingly, the viscosity and boiling points of the ERBS fuel were higher than those for more fully refined Jet-A fuel. In addition, the aromatic content of the ERBS fuel was more than double the amount (per volume) of that of the Jet-A fuel.

Research Radiometer

The research radiometer, a commercially available unit is shown in figure 7. The unit was supplied with an indium antimonide detector coupled to a two-segment, circular variable filter to provide spectral response over a range of wavelengths from 1.55 to 5.5 micrometers. The two-segment, circular variable filter is of the interference type, in which a thin film of semiconductor material is deposited on a substrate, resulting in a narrow-band transmission filter. The first segment covered the 1.55- to 3.0-micrometer spectrum with an average half bandwidth of 1.80 percent. The second segment

covered the 3.0- to 5.5-micrometer spectrum with an average half bandwidth of 1.02 percent. The half bandwidth of the filter is a measure of its spectral selectivity. For example, given a half bandwidth of 1 percent centered around 4 micrometers of wavelength, the filter will principally transmit radiant energy from 3.98 to 4.02 micrometers. Rotation of the filter was controlled by a microprocessor built into the system. Scan rate, filter position, and dwell time were preprogrammed to optimize data acquisition.

The research radiometer was used in conjunction with a front-surfaced mirror mounted on a motor-driven translator as shown in figure 8. This arrangement permitted optical access to all three viewing ports without moving the research radiometer. An analog position control was set to provide accurate optical alinement. Control of both the translator and the research radiometer was maintained from a remotely located control room.

TABLE I.—FUEL CHARACTERISTICS

Specifications	Jet-A	ERBS
ASTM distillation, K:		
Initial boiling point	411	435
10 percent evaporated	451	461
50 percent evaporated	479	488
90 percent evaporated	517	552
Final boiling point	531	601
Specific gravity at 289 K	0.8142	0.8381
Freezing point, K	226	244
Viscosity at 250 K, m^2/sec	5×10^{-6}	7.2×10^{-6}
Net heat of combustion, J/g	43 304	42 585
Hydrogen, percent by weight	13.9	12.9
Aromatics, percent by volume	17.2	35.0
Sulfur (total), percent by weight	0.020	0.085

Calibration

The equation governing instrument calibration is

$$i_{\lambda,eff} = \frac{V_o}{K_s}$$

where $i_{\lambda,eff}$ is the effective measured radiance, V_o is the instrument output voltage, and K_s is the instrument response coefficient. In calibrating from a blackbody source of known temperature the equation is rearranged as follows:

$$K_s = \frac{V_o}{i_{\lambda,eff}}$$

The effective measured radiance is defined as

$$i_{\lambda,eff} = \int_{\lambda_1}^{\lambda_2} R_\lambda i_{\lambda b} d\lambda$$

where R_λ is the normalized product of detector response and filter transmission and λ_1 and λ_2 are determined from the filter halfbandwidth.

These equations can be solved to determine K_s at each measured wavelength. Calibration was done at two temperatures to ensure that K_s would be valid over the temperature range of interest.

The radiometric system was calibrated by using a

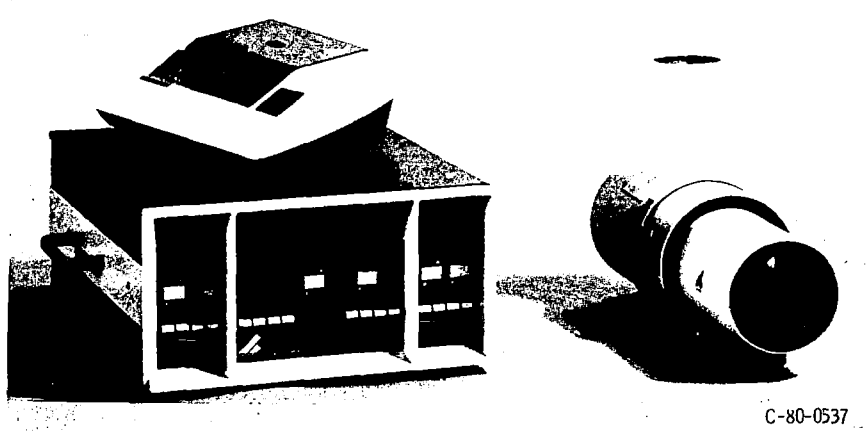

Figure 7. - Spectral radiometer.

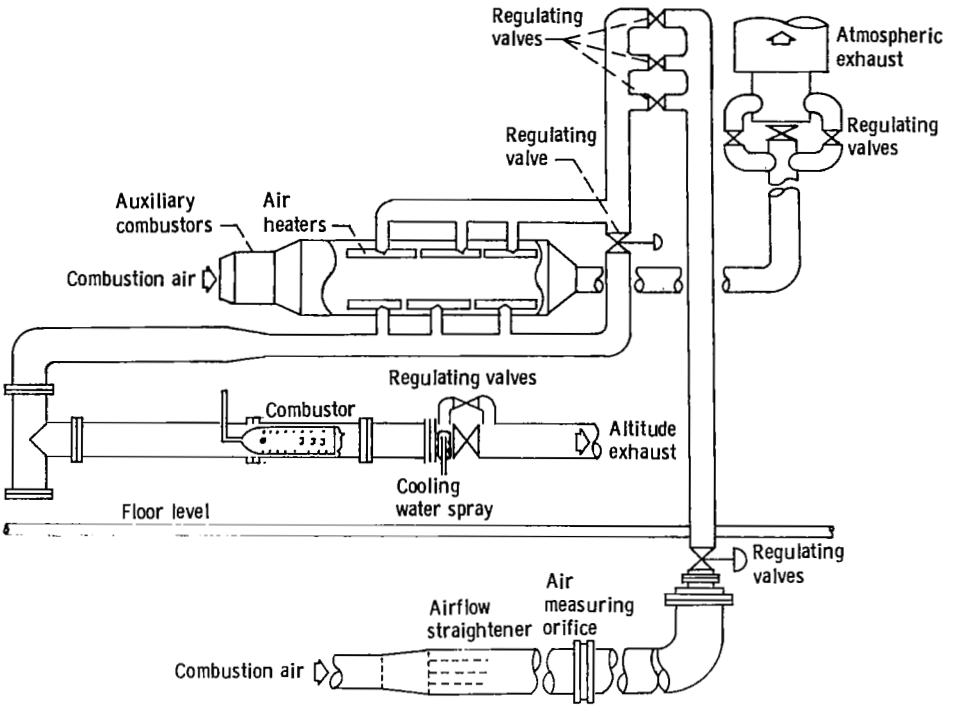

Figure 5. - Test facility and auxiliary equipment.

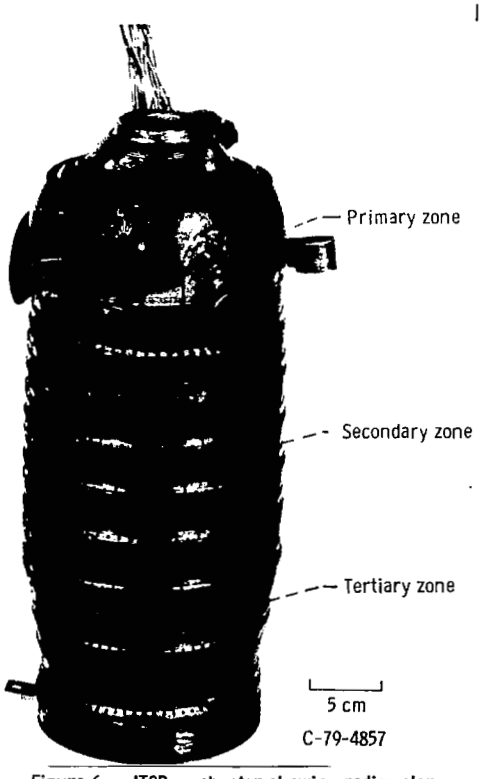

Figure 6. - JT8D combustor showing radiometer observation ports.

Fuels

The characteristics of the two fuels used in this investigation are given in table I. The specifications for the experimental referee broadened-specification (ERBS) aviation turbine fuel were established in reference 15. It was proposed that such a fuel could be produced from the available petroleum stocks without excessive processing costs. Accordingly, the viscosity and boiling points of the ERBS fuel were higher than those for more fully refined Jet-A fuel. In addition, the aromatic content of the ERBS fuel was more than double the amount (per volume) of that of the Jet-A fuel.

Research Radiometer

The research radiometer, a commercially available unit is shown in figure 7. The unit was supplied with an indium antimonide detector coupled to a two-segment, circular variable filter to provide spectral response over a range of wavelengths from 1.55 to 5.5 micrometers. The two-segment, circular variable filter is of the interference type, in which a thin film of semiconductor material is deposited on a substrate, resulting in a narrow-band transmission filter. The first segment covered the 1.55- to 3.0-micrometer spectrum with an average half bandwidth of 1.80 percent. The second segment

covered the 3.0- to 5.5-micrometer spectrum with an average half bandwidth of 1.02 percent. The half bandwidth of the filter is a measure of its spectral selectivity. For example, given a half bandwidth of 1 percent centered around 4 micrometers of wavelength, the filter will principally transmit radiant energy from 3.98 to 4.02 micrometers. Rotation of the filter was controlled by a microprocessor built into the system. Scan rate, filter position, and dwell time were preprogrammed to optimize data acquisition.

The research radiometer was used in conjunction with a front-surfaced mirror mounted on a motor-driven translator as shown in figure 8. This arrangement permitted optical access to all three viewing ports without moving the research radiometer. An analog position control was set to provide accurate optical alinement. Control of both the translator and the research radiometer was maintained from a remotely located control room.

TABLE I.—FUEL CHARACTERISTICS

Specifications	Jet-A	ERBS
ASTM distillation, K:		
Initial boiling point	411	435
10 percent evaporated	451	461
50 percent evaporated	479	488
90 percent evaporated	517	552
Final boiling point	531	601
Specific gravity at 289 K	0.8142	0.8381
Freezing point, K	226	244
Viscosity at 250 K, m^2/sec	5×10^{-6}	7.2×10^{-6}
Net heat of combustion, J/g	43 304	42 585
Hydrogen, percent by weight	13.9	12.9
Aromatics, percent by volume	17.2	35.0
Sulfur (total), percent by weight	0.020	0.085

Calibration

The equation governing instrument calibration is

$$i_{\lambda,eff} = \frac{V_o}{K_s}$$

where $i_{\lambda,eff}$ is the effective measured radiance, V_o is the instrument output voltage, and K_s is the instrument response coefficient. In calibrating from a blackbody source of known temperature the equation is rearranged as follows:

$$K_s = \frac{V_o}{i_{\lambda,eff}}$$

The effective measured radiance is defined as

$$i_{\lambda,eff} = \int_{\lambda_1}^{\lambda_2} R_\lambda i_{\lambda b} d\lambda$$

where R_λ is the normalized product of detector response and filter transmission and λ_1 and λ_2 are determined from the filter halfbandwidth.

These equations can be solved to determine K_s at each measured wavelength. Calibration was done at two temperatures to ensure that K_s would be valid over the temperature range of interest.

The radiometric system was calibrated by using a

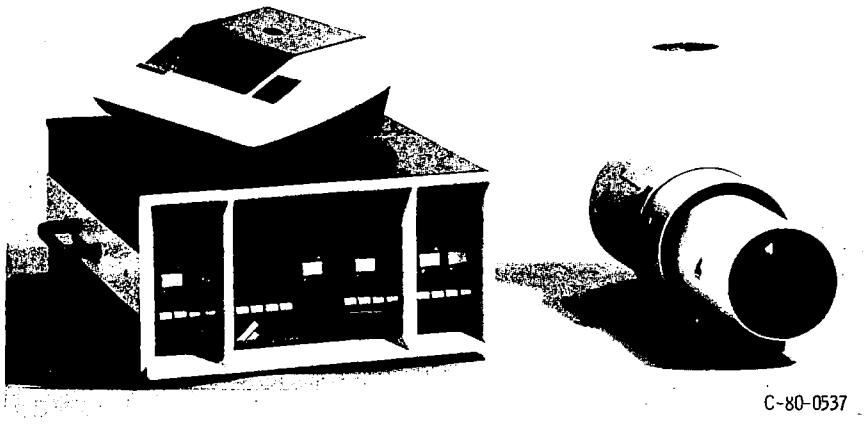

Figure 7. - Spectral radiometer.

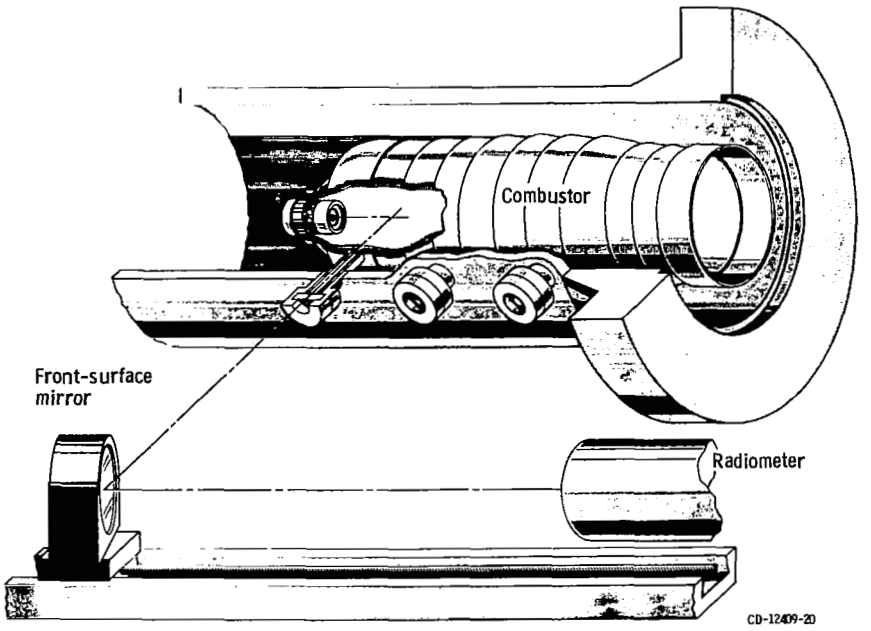

Figure 8. - Schematic drawing of spectral radiometer optical path.

blackbody source capable of temperatures to 1273 K. The optical system, which included sapphire windows and a front-surface mirror, was arranged in precise geometric alinement between the blackbody source and the spectral detector. The detector was located 114 centimeters from the blackbody source, and for all measurements no attempt was made to purge atmospheric carbon dioxide and water vapor from the viewing path.

Gas Analysis

The exhaust gas was analyzed for concentrations of carbon dioxide, carbon monoxide, unburned hydrocarbons, and oxides of nitrogen in accordance with the recommendations set forth in reference 16. A gas analysis fuel-air ratio could be determined from a carbon balance of the measured gaseous emissions. To test if the gas sample was representative, this fuel-air ratio was compared with that calculated from fuel and airflow measurements. The agreement was within ± 15 percent, an indication that the sample was representative.

Results and Discussion

Spectral measurements of flame radiance in a JT8D combustor were taken over a range of operating conditions with both Jet-A and ERBS fuel. From these spectral measurements local values of soot concentration and flame temperature were determined in accordance with the procedure detailed in the section Analysis. The results are summarized in table II for the full range of operating conditions investigated.

Comparisons between Jet-A and ERBS fuel were made at four of the seven operating points investigated. The operating point listed in table II as 1 matched the inlet-air temperature and fuel-air ratio of a JT8D engine operating at a power level between 30 to 50 percent of full power. The inlet-air pressure was lower than appropriate to fully simulate this engine power level. However, these conditions are the closest approximation of high-power engine conditions for which a fuels comparison could be made. The lower power conditions, points 2 to 4, simulated the inlet-air temperature and pressure of a JT8D engine at idle settings. Operating point 3 exactly simulated the idle fuel-air ratio, with points 2 and 4 representing parametric variations.

In the following sections the units of radiance used in the spectral curves are in terms of spectral intensity, which is defined as energy emitted per unit time per wavelength interval around λ per unit solid angle per projected area. The hemispherical spectral emissive power is π times the spectral intensity.

Effect of Fuel Type

The effect of fuel type on spectral flame radiance at operating condition 1 is shown in figure 9. ERBS

TABLE II.—DATA SUMMARY

Operating point	Inlet-air pressure, MPa	Inlet-air temperature, K	Fuel type	Fuel-air ratio	Primary zone		Secondary zone		Tertiary zone	
					Flame temperature, K	Soot concentration, mg/m^3	Flame temperature, K	Soot concentration, mg/m^3	Flame temperature, K	Combustion efficiency, percent
1	0.34	533	Jet-A	0.0155	1227	5700	2090	650	1345	99.7
			ERBS	.0155	1347	4800	2412	575	1962	99.7
2	.28	400	Jet-A	.006	1255	820	1096	---	672	90.2
			ERBS	.006	1551	1900	1095	---	769	97.2
3	.28	400	Jet-A	.0074	1246	910	1317	---	783	91.8
			ERBS	.0074	1362	763	1160	---	878	98.6
4	.28	400	Jet-A	.009	1278	880	1518	---	866	93.3
			ERBS	.009	1467	1500	1950	---	1094	98.1
5	.34	700	Jet-A	.0155	1376	6218	2125	963	1435	99.9
6	.34	700	Jet-A	.0125	1334	6450	2044	475	1345	99.9
7	1.03	533	Jet-A	.0155	---	---	2440	2770	---	99.9

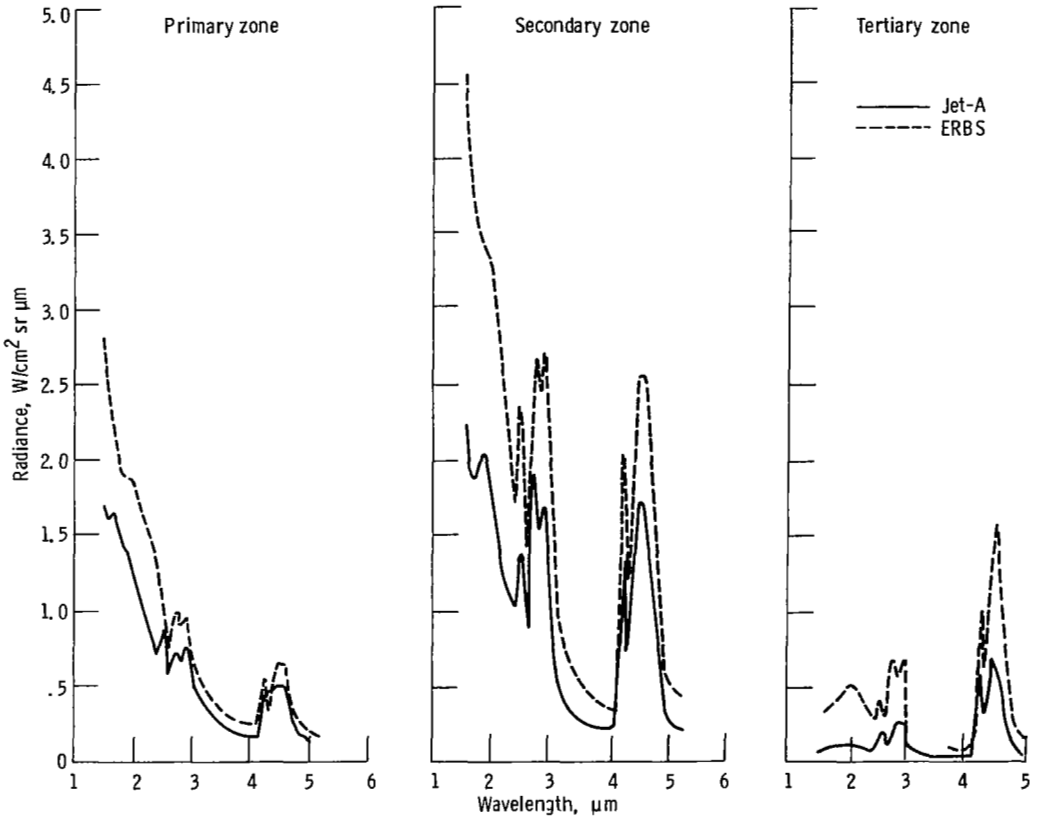

Figure 9. - Spectral flame radiance as a function of fuel type for inlet-air pressure of 0.34 MPa, inlet-air temperature of 533 K, and fuel-air ratio of 0.0155.

fuel combustion resulted in increased spectral flame radiance at all observation points in the combustor. These higher radiance levels ranged from 220 to 17 percent greater than the Jet-A radiance levels. From inspection of table II these higher radiance levels can be attributed to higher flame temperatures. For example, the flame temperature increased from 2090 K with Jet-A to 2412 K with ERBS fuel in the

secondary zone of the combustor while soot concentration decreased from 650 mg/m^3 to 575 mg/m^3. The higher flame temperatures may have promoted higher soot oxidation rates and hence lower soot concentrations.

These higher flame temperatures may be a result of the difference between Jet-A and ERBS fuel properties. (Fuel properties are tabulated in table I). Two of the properties in particular appear to be the main causes. First, the higher viscosity of the ERBS fuel should result in larger fuel droplets with more nearly stoichiometric combustion of the fuel. Second, the higher distillation points of the fuel may result in combustion further downstream of the fuel nozzle. This second argument is more likely to be true at richer fuel-air ratio conditions.

The spectral curves shown in figure 9 were integrated with respect to wavelength to identify the radiant energy contributed by the various emitters as shown in figure 10. Each contributor was identified as noted in the section Analysis. Soot was the major contributor to total flame radiation. ("Total" here is defined as the spectral region from 1.55 to 5.5 μm.) Typically soot contributed from 80 to 70 percent of the total flame radiation in the primary zone, from 70 to 50 percent of the total flame radiation in the secondary zone, and from 50 to 35 percent of the total flame radiation in the tertiary zone. The higher values of total radiation intensity with ERBS fuel were primarily caused by increased soot particle radiation. This might appear somewhat surprising since, as previously noted, the soot concentrations were reduced. However, the temperature of the soot particles was greatly increased; and as radiation is proportional to the fourth power of temperature, the soot radiation intensities were understandably increased.

The effect of fuel type on spectral flame radiance at low-power operating conditions, points 2 and 3, is displayed in figures 11 and 12. These figures demonstrate that the effect of fuel type is very sensitive to the engine operating condition. Unlike for operating condition 1 (fig. 9) an increase in spectral flame radiance was not always recorded with the ERBS fuel. As shown in figure 11 the secondary-zone radiance was unaffected by a change in fuel type. As shown in figure 12 the secondary-zone radiance decreased during the combustion of ERBS fuel.

Possible explanations for these phenomena can be advanced. The lack of any change in the secondary-zone radiance levels of figure 11 can be attributed to a lack of combustion occurring in the secondary zone at this very lean fuel-air ratio condition. All combustion could have occurred in the primary zone, and by the time the combustion gases reached the secondary zone the exothermic reactions would have been completed. In figure 12 the decrease in spectral radiance during the combustion of ERBS fuel can be attributed to a change in the fuel spray quality. Figure 12 depicts a slightly higher fuel-air ratio than figure 11. This requires a greater fuel nozzle pressure drop (because of the higher fuel flow), which may result in finer atomization of the fuel spray. This would cause the most intense burning to occur close to the fuel nozzle, given sufficient quantities of oxygen. This more intense combustion would require less time to go to completion than the lower temperature Jet-A combustion. Therefore in the secondary zone of figure 12 some combustion may still be occurring with Jet-A, whereas with ERBS fuel most of the combustibles have been consumed.

A similar effect was observed by Reeves in reference 1. Visual observations by Reeves showed that residual fuels had a short, intense flame mainly confined to the space immediately downstream of the fuel nozzle. Flames produced by distillate fuels similar to Jet-A were less intense and more uniform and extended farther down the combustor.

Over the range of operating conditions investigated it appears that the effect of burning a broadened specification fuel such as ERBS is very much dependent on the combustor operating conditions. But generally it was determined that for

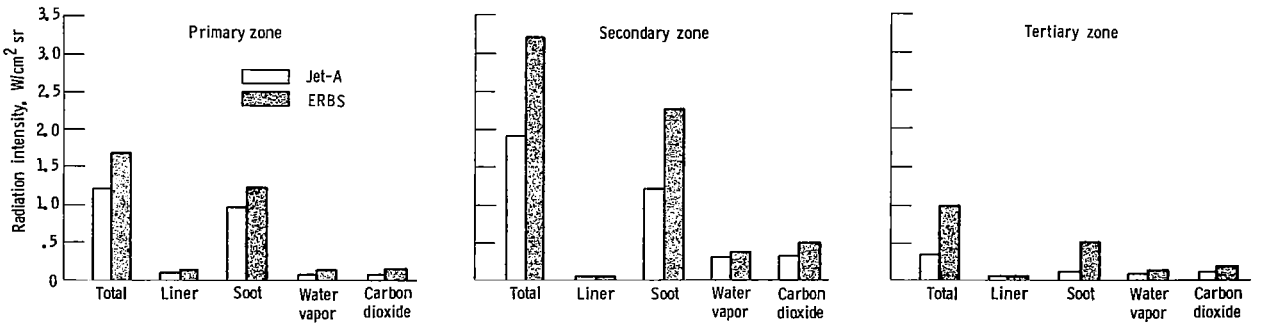

Figure 10. - Radiant energy contributed by various sources in observed spectral region.

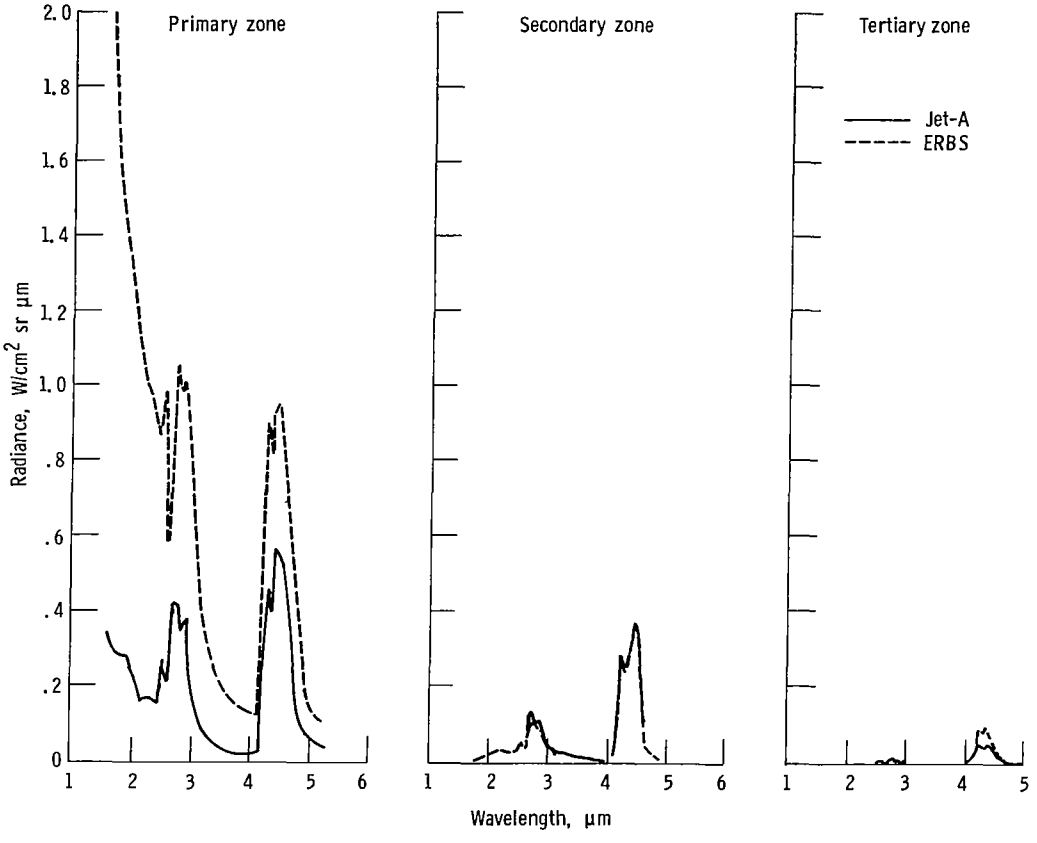

Figure 11. - Spectral flame radiance as a function of fuel type and wavelength for inlet-air pressure of 0.28 MPa, inlet-air temperature of 400 K, and fuel-air ratio of 0.006.

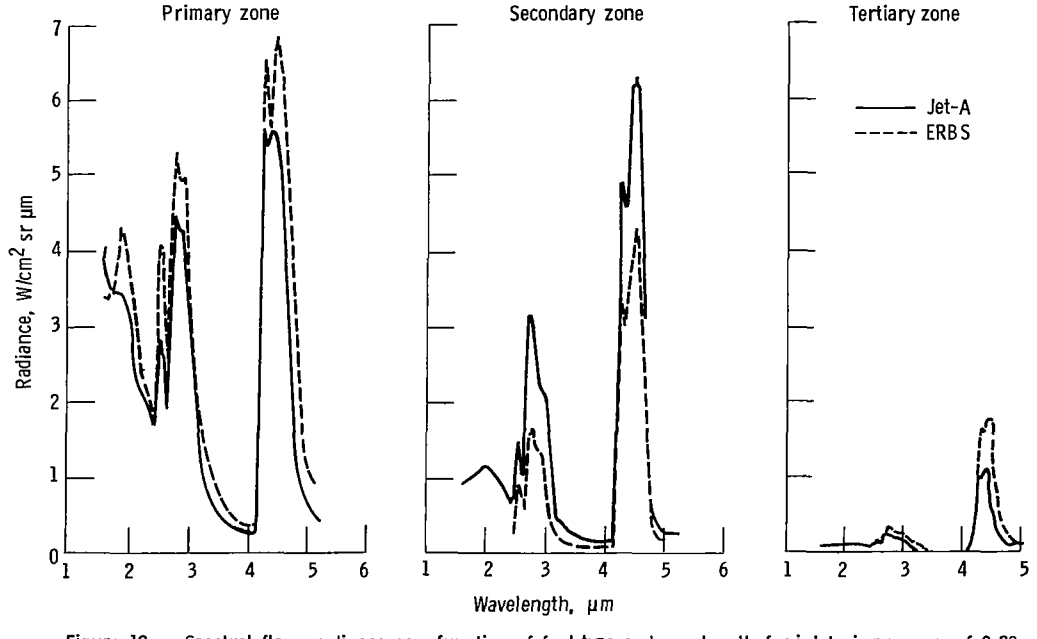

Figure 12. - Spectral flame radiance as a function of fuel type and wavelength for inlet-air pressure of 0.28 MPa, inlet-air temperature of 400 K, and fuel-air ratio of 0.0074.

the operating conditions investigated, ERBS fuel will produce increased flame temperatures somewhere in the combustor. At the operating condition (1) most closely approximating high engine power levels, higher flame temperatures were produced throughout the combustor.

These higher flame temperatures were beneficial to the combustion process. Gas analysis measurements at the exhaust plane of the combustor indicated an increase in combustion efficiency at all the low-power operating conditions, points 2 to 4 in table II. The combustion efficiencies recorded during the burning of ERBS fuel were typically 6 to 7 percent higher than those with Jet-A fuel. Apparently oxidation of unburned hydrocarbons and carbon monoxide was promoted by the higher flame temperatures.

Effect of Fuel-Air Ratio

The effect of fuel-air ratio on spectral flame radiance resulting from the combustion of Jet-A fuel at operating conditions 5 and 6 is shown in figure 13. The primary-zone spectrum was not significantly affected by a change in the fuel-air ratio from 0.0125 to 0.0155. However, the secondary- and tertiary-zone spectra were increased at the higher fuel-air ratio. Even at the low-power conditions the fuel-air ratio had almost no effect on the primary-zone spectral radiance when Jet-A fuel was burned. From table II at the fuel-air ratios corresponding to 0.06, 0.074, and 0.09 (low-power conditions) the flame temperature varied only by a maximum of 32 kelvins, and the soot concentrations were all within ±6 percent of an average value of 870 mg/m^3.

This stands in marked contrast to the ERBS fuel data. At the same conditions the flame temperature varied a maximum of 189 kelvins with the soot concentration varying as much as 1137 mg/m^3. This variation may be caused by the intense portion of the ERBS fuel flame moving to different axial locations in the combustor as the fuel rate is varied. As mentioned previously distillate fuel flames were observed by Reeves to be more uniform and would therefore be much less sensitive to fuel-air ratio variations in the primary zone.

Effect of Inlet-Air Pressure

The effect of inlet-air pressure on spectral flame radiance in the secondary zone of the combustor is shown in figure 14. The increase in inlet-air pressure from 0.34 MPa to 1.03 MPa resulted in a large increase in the flame spectrum. This was attributed to an increase in both flame temperature and soot concentration. The flame temperature increased from 2040 K to 2440 K, and the soot concentration increased from 650 mg/m^3 to 2770 mg/m^3.

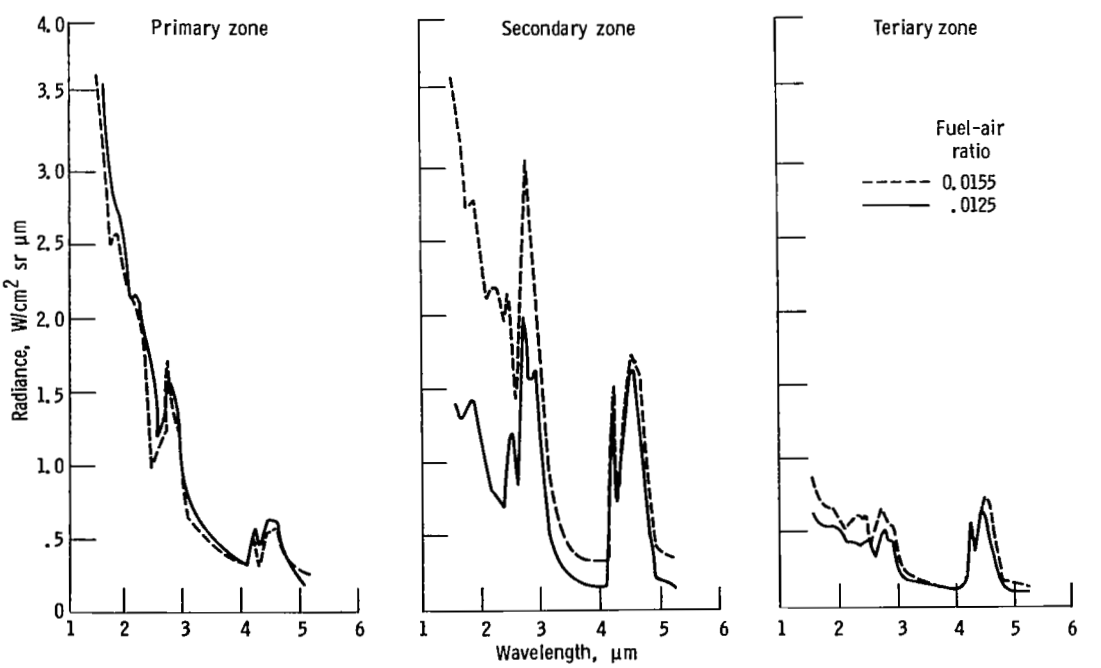

Figure 13. - Spectral flame radiance as a function of fuel-air ratio and wavelength for Jet-A fuel at inlet-air pressure of 0.34 MPa and inlet-air temperature of 700 K.

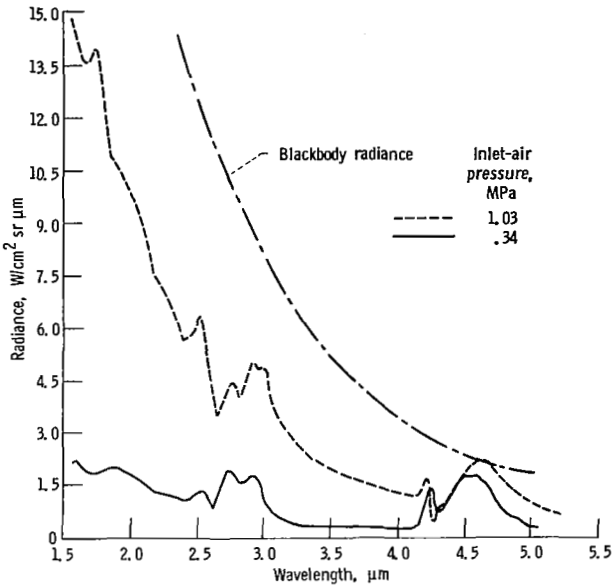

Figure 14. - Spectral flame radiance in secondary zone of combustor as a function of inlet-air pressure and wavelength for Jet-A fuel at inlet-air temperature of 533 K and fuel-air ratio of 0.0155.

The spectral radiance of a blackbody at 2440 K is shown in the same figure. (This temperature corresponds to the flame temperature for the high-pressure condition.) The high-pressure flame radiance is an appreciable portion of the blackbody radiance, typically around 35 to 50 percent. This is considerably greater than the low-pressure radiance, yet it indicates that the spectral radiance (i.e., total flame radiation) may increase still further at even higher pressures.

Concluding Remarks

The effect of a number of variables on flame radiation in a JT8D can combustor has been observed. Unfortunately none of these variables has been mapped as fully as is desirable, especially in regard to pressure. Future work will address this need. Nevertheless, from the information obtained thus far it can be seen that the nonintrusive measurement technique employed in this investigation can provide insight as to the effect of combustor operating variables on flame temperature and soot concentration levels within the combustor.

Summary of Results

Emission measurements were taken of spectral flame radiance from which both flame temperature and soot concentration could be analytically determined. From this the following results were obtained:

1. Combustion of ERBS fuel, a fuel with both a higher viscosity and a higher boiling point than conventional Jet-A fuel, generally resulted in higher levels of flame radiance than did Jet-A. This phenomenon was usually attributed to increased flame temperatures along the whole length of the combustor.

2. The effect of fuel type was quite sensitive to combustor operating condition. At one isolated operating point flame radiance in the secondary zone of the combustor was higher for Jet-A fuel than for the less volatile, more viscous ERBS fuel.

3. Soot was the major contributor to total flame radiation for the observed spectral region from 1.55 to 5.5 micrometers of wavelength. Typically soot contributed from 80 to 70 percent of the total flame radiation in the primary zone, from 70 to 50 percent of the total flame radiation in the secondary zone, and from 50 to 35 percent of the total flame radiation in the tertiary zone.

4. With Jet-A fuel an increase in the fuel-air ratio had no effect on the primary-zone spectral radiance but did increase the spectral radiance in the secondary and tertiary zones. With ERBS fuel the primary-zone spectral radiance was very sensitive to the fuel-air ratio.

5. An increase in inlet-air pressure from 0.34 MPa to 1.03 MPa resulted in an increase in flame temperature from 2040 K to 2440 K and an increase in soot concentration from 650 mg/m^3 to 2770 mg/m^3 with Jet-A fuel.

Lewis Research Center
National Aeronautics and Space Administration
Cleveland, Ohio, September 11, 1980

References

1. Reeves, D.: Flame Radiation in an Industrial Gas Turbine Combustion Chamber. NGTE-Memo.-285, National Gas Turbine Establishment (England), 1956.

2. Moses, C. A.; and Naegeli, D. W.: Fuel Property Effects on Combustion Performance. ASME Paper 79-GT-178, Mar. 1979.

3. Schirmer, R. M.; and Quigg, H. T.: High Pressure Combustor Studies of Flame Radiation as Related to Hydrocarbon Structure. Rep. 3952-65R, Phillips Petroleum Co., 1965. (AD-617191).

4. Jackson, T. A.; and Blazowski, W. S.: Fuel Hydrogen Content as an Indicator of Radiative Heat Transfer in an Aircraft Gas Turbine Combustor, AFAPL-TR-79-2014, Air Force Aero Propulsion Lab., 1979. (AD-A067709).

5. Beer, J. M.; and Siddal, R. G.: Radiative Heat Transfer in Furnaces and Combustors. ASME Paper 72-WA/HT-29, 1972.

6. Sarofim, A. F.; and Hottel, H. C.: Radiative Transfer In Com-bustion Chambers: Influence of Alternative Fuels. Sixth International Heat Transfer Conference, Vol. 6—Keynote Papers. Hemisphere Publishing Corp., 1978, pp. 199–217.

7. Norgren, C. T.: Determination of Primary-Zone Smoke Concentrations from Spectral Radiance Measurements in Gas Turbine Combustors. NASA TN D-6410, 1971.

8. Norgren, C. T.; and Ingebo, R. D.: Spectral Radiance Measure-ments and Calculated Soot Concentrations Along the Length of an Experimental Combustor. NASA TM X-3394, 1976.

9. Edward, D. K.: Molecular Gas Band Radiation. Advances in Heat Transfer, Vol. 12. T. F. Irvine and J. P. Hartnett, eds., Academic Press, 1976, pp. 115–193.

10. Miller, E. C.; et al.: Radiation from Laboratory Scale Jet Combustor Flames. Rep. 1526-56R, Phillips Petroleum Co., 1956.

11. Foster, P. J.: Calculation of the Optical Properties of Dispersed Phases. Combust. Flame, Vol. 7, no. 3, Sept. 1963, pp. 277–282.

12. Godridge, A. M.; and Hammond, E. G.: Emissivity of a Very Large Residual Fuel Oil Flame. Twelfth Symposium (International) on Combustion. F. Kaufman, ed., The Combustion Institute, 1969, pp. 1219–1228.

13. Liebert, C. H.; and Hibbard, R. R.: Spectral Emittance of Soot. NASA TN D-5647, 1970.

14. Howarth, C. R.; Foster, P. J.; and Thring, M. W.: The Effect of Temperature on the Extinction of Radiation by Soot Particles. Third International Heat Transfer Conference, Vol. 5 American Institute of Chemical Engineers, 1966, pp. 122–128.

15. Longwell, J. P., ed.: Jet Aircraft Fuels Technology. NASA CP-2033, 1978.

16. Procedure for the Continuous Sampling and Measurement of Gaseous Emissions from Aircraft Turbine Engines. Aerospace Recommended Practice 1256, Society of Automotive Engineers, Inc., Oct. 1971.

1. Report No.	2. Government Accession No.	3. Recipient's Catalog No.
NASA TP-1722		

4. Title and Subtitle	5. Report Date
SPECTRAL FLAME RADIANCE FROM A TUBULAR-CAN COMBUSTOR	February 1981
	6. Performing Organization Code 505-32-32
7. Author(s)	8. Performing Organization Report No.
Russell W. Claus	E-509
	10. Work Unit No.
9. Performing Organization Name and Address	
National Aeronautics and Space Administration Lewis Research Center Cleveland, Ohio 44135	11. Contract or Grant No.
	13. Type of Report and Period Covered
12. Sponsoring Agency Name and Address	Technical Paper
National Aeronautics and Space Administration Washington, D.C. 20546	14. Sponsoring Agency Code

15. Supplementary Notes

16. Abstract

An experimental investigation was conducted to determine the effects of fuel type, fuel-air ratio, and inlet-air pressure on the spectral flame radiance emanating from a JT8D can combustor. Spectral radiance measurements from 1.55 to 5.5 micrometers of wavelength were recorded and analyzed to determine soot concentration and flame temperature at various axial locations in the combustor. Two fuels differing in volatility, viscosity, and chemical composition were used in this investigation.

17. Key Words (Suggested by Author(s))	18. Distribution Statement
Flame radiation Alternative fuels Spectral radiance	Unclassified - unlimited STAR Category 07

19. Security Classif. (of this report)	20. Security Classif. (of this page)	21. No. of Pages	22. Price*
Unclassified	Unclassified	15	A02

* For sale by the National Technical Information Service, Springfield, Virginia 22161

NASA-Langley, 1981